Site-Specific Labeling of Supercoiled DNA at the A+T Rich Sequences†

Vladimir N. Potaman,*,‡ Alexander Y. Lushnikov,§ Richard R. Sinden,‡ and Yuri L. Lyubchenko*,§

Center for Genome Research, Institute of Biosciences and Technology, Texas A&M University System Health Sciences Center, Houston, Texas 77030-3303, and Departments of Biology and Microbiology, Arizona State University, Tempe, Arizona 85287-2701

Received July 3, 2002; Revised Manuscript Received September 6, 2002

ABSTRACT: Progress in structural biology studies of supercoiled DNA and its complexes with regulatory proteins depends on the availability of reliable and routine procedures for site-specific labeling of circular molecules. For this, we made use of oligonucleotide uptake by plasmid DNA under negative superhelical tension. Subsequent circularization of the oligonucleotide label facilitated by an oligonucleotide scaffold results in its threading between the two strands of duplex DNA. Several lines of evidence, including direct AFM mapping of the label, show that the circular oligonucleotide is stably localized at its target, an A+T rich region. The specific binding mode when the oligonucleotide threads the double helix results in a DNA kink that tends to occupy an apical position in a plectonemically wound supercoiled DNA, similar to the positioning of an A-tract bend. Site-specific labels may allow visualization techniques, such as electron and atomic force microscopies, to reliably map protein binding sites, identify local alternative structures in supercoiled DNA, and monitor structural dynamics of DNA molecules in real time. Site-specific oligonucleotide reactions with DNA may also have application in biotechnology and gene therapy.

Progress in structural biology studies of supercoiled DNA and its complexes with regulatory proteins depends on the availability of reliable and routine procedures for site-specific labeling of circular molecules. Site-specific labels in superhelical DNA are needed to map local structures such as bent DNA, cruciform DNA, and intramolecular triplex (*1*−*3*) as well as protein binding sites (*4*, *5*). Site-specific plasmid modification is useful for DNA immobilization at the AFM support for further visualization (*6*). Several site-specific DNA labeling approaches that use oligodeoxynucleotides (ODNs)[1] have been proposed. A triplex-forming oligodeoxynucleotide (TFO) was hybridized at a homopurine-homopyrimidine (Pu·Py) sequence, cross-linked to DNA through a psoralen moiety at the TFO 5′-end, and visualized by a biotin−streptavidin complex at the ODN 3′-end (*7*). Two approaches were described for site-specific ODN hybridization followed by its circularization. The TFO was bound to DNA and then ligated into a circular form using a scaffold ODN bound at extended ends of the TFO (*8*). The circularized TFO, a padlock, was catenated with plasmid DNA, but the label was site-specific only under the conditions of stable triplex formation; otherwise, it could move away from the hybridization position (*8*−*10*). In another approach, the Pu·Py sequence was unwound by strand invasion of two peptide nucleic acid (PNA) oligomers targeted to the Pu strand (*11*, *12*). The unpaired Py strand served as a scaffold for hybridizing the ends of an ODN that was circularized by ligation. The circularized ODN, an earring, was threaded and catenated between the two strands of duplex DNA, could not dissociate, and was, therefore, truly site-specific. The applicability of all three labeling techniques described above so far has been limited to Pu·Py rich sequences. In recent work, selected regions in random sequence DNA were targeted by simultaneous strand invasion of a pair of pseudocomplementary PNAs (*13*). Such a strategy may potentially be developed into a powerful approach for site-specific DNA labeling by PNA oligomers, especially if their association with each other is reduced to an acceptable level. Supercoiled DNA may also be labeled by nick translation from restriction sites where, under suboptimal conditions, enzymes cleave only one instead of both strands (*1*). DNA labeling by this technique is not very precise, as a biotin−streptavidin label has been shown to incorporate within several hundred base pairs of the nick site.

One attractive possibility for expanding the repertoire of DNA sequences targeted for site-specific labeling is to use the ability of superhelical DNA to take up homologous single-stranded fragments (*14*−*17*). Single-strand uptake is facilitated by increasing temperature and negative superhelicity, factors that promote DNA unwinding. We reasoned that the easily unwound A+T rich sequences, termed DNA unwinding elements (*18*−*21*), might be convenient targets for ODN hybridization and further circularization. The extent of DNA unwinding in the A+T rich regions can be

† This work was supported by Grants GM 62235 (NIH) and DBI-0070356 (NSF).

* To whom correspondence should be addressed. V.N.P.: phone, (713) 677-7675; fax, (713) 677-7689; e-mail, vpotaman@ibt.tamu.edu. Y.L.L.: phone, (480) 965-8430; fax, (480) 965-0098; e-mail, yuri.lyubchenko@asu.edu.

‡ Texas A&M University System Health Sciences Center.

§ Arizona State University.

[1] Abbreviations: nt, nucleotide; ODN, oligodeoxynucleotide; TFO, triplex-forming oligonucleotide; Pu·Py, homopurine-homopyrimidine; σ, superhelical density; PNA, peptide nucleic acid; CAA, chloroacetaldehyde; EtBr, ethidium bromide; AFM, atomic force microscopy.

10.1021/bi026402w CCC: $22.00
Published on Web 10/11/2002

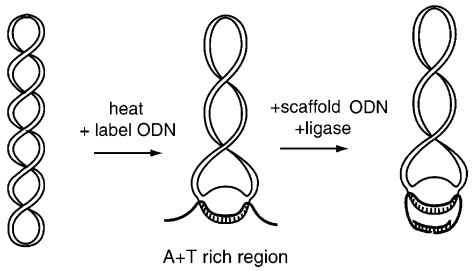

FIGURE 1: Schematics of supercoiled DNA labeling by ODN circularization at the A+T rich sequences. Torsional stress and an elevated temperature transiently open an A+T rich sequence in supercoiled DNA and allow hybridization of a label ODN. After addition of the scaffold ODN and ligase, the reaction mixture is adjusted to an optimal ligation temperature.

manipulated by changes in plasmid superhelicity, ionic strength, and temperature. Circularized ODNs are expected to thread double-stranded DNA and therefore be restricted to their hybridization positions unless strand separation in the flanking DNA sequences occurs. One example of an appropriate unwinding element is a 97 bp long, 76% A+T rich region adjacent to the β-lactamase gene that is present in most cloning vectors.

Our approach is schematically shown in Figure 1. To test the feasibility of ODN circularization at this sequence, we used a pUC-based plasmid at a superhelical density as isolated from *Escherichia coli* ($\sigma \sim -0.05$). At elevated temperatures (65 °C), an internal part of the label ODN hybridizes with the central part of the unwound A+T rich region. Another ODN serves as a scaffold for ligation of the label ODN after its threading through a transiently unpaired DNA region. Several lines of evidence, including direct AFM mapping of the label, are presented to show that the circular ODN is stably localized at its target in the A+T rich region. Streptavidin bound to the biotin-modified ODN may serve as an internal marker in the circular DNA molecule as well as a means of DNA attachment to the modified mica support in atomic force microscopy. Site-specific ODN reactions may also be used in various gene therapy applications.

EXPERIMENTAL PROCEDURES

Materials. Plasmid pEV70 is a pUC derivative with a 70 bp polylinker sequence. Supercoiled plasmid was isolated from the HB101 *E. coli* strain by alkaline lysis followed by purification with a CsCl density gradient. ODNs were synthesized and purified from a denaturing gel by Integrated DNA Technologies (Coralville, IA). ODN V was internally modified via biotin−dT incorporation during synthesis. T4 and *Taq* DNA ligases, T4 polynucleotide kinase, and restriction enzymes, all from New England Biolabs (Beverly, MA), were used according to the manufacturer's protocols. DNA polymerases *KlenTaq*1 and *Pfu* were from Ab Peptides (St. Louis, MO) and Stratagene (La Jolla, CA), respectively. Topoisomerase I-containing nuclear extract from HeLa cells was prepared as described previously (*22*).

DNA Topoisomer Preparation and Chemical Probing of the A+T Rich Region. Supercoiled DNA topoisomer fractions were generated by incubating 5 μg of plasmid DNA with 8 μL of topoisomerase I-containing nuclear extract from HeLa cells in the presence of appropriate concentrations of ethidium bromide (EtBr). Superhelical densities of resultant topoisomer fractions were calculated with the equation $\sigma = -10.5\tau/N$, where N is the number of base pairs in the plasmid and τ is the number of superhelical turns determined by the band counting method after topoisomer separation in agarose gel in the presence of chloroquine (*23*). For chemical probe analysis of unpaired regions in supercoiled plasmids (*23*), 0.25 μg of DNA in 40 μL of 0.5× TEN buffer [5 mM Tris-HCl, 25 mM NaCl, and 0.5 mM EDTA (pH 7.4)] was treated with 0.5% chloroacetaldehyde (CAA) for 8 min at 37 °C, and reactions were terminated by diethyl ether extraction. After ethanol precipitation, 0.1 μg of DNA was used for primer extension with a Stoffel fragment of Taq polymerase that terminates synthesis at the chemically modified bases. Products of primer extension and DNA sequencing with the same primers and a mixture of *KlenTaq*1 and *Pfu* polymerases (*24*) were separated on a 7% sequencing gel which was exposed to a PhosphoImager screen for analysis of reactive sites by ImageQuant software (Molecular Dynamics).

Table 1: Oligonucleotide Sequences[a]

ODN I	TCCATGGCAA CTGTAACGCT ACATGAGATT ATCAAAAAGG
	ATCTTCACCT AGATCCTTTT AATCACTATT CGATCACTAC GATCGT
ODN II	CACTACGATC GTTCCATGGC ATACATTATC AAAAAGGATC
	TTCACCTAGA TCCTTCACCA GTCGAC
ODN III	CACTACGATC GTTCCATGGC ATACAGGATC TTCACCTAGA
	TCCTTCACCA GTCGAC
ODN IV	ACTACGATCG TTCCATGGCA TACATTATCA AAAAGGATCT
	TCACCTAGAT CCTTCACCAG TCGACC
ODN V	CACTACGATC GTTCCAT*GG CATACATTAT CAAAAAGGAT
	CTTCACCTAG ATCCTTCACC AGTCGAC
ODN VI	ACGATCGTAG TGGTCGACTG G

[a] Parts of ODN sequences complementary to the unwound DNA strand are underlined. T* in ODN V is a biotinylated thymine.

ODN Hybridization and Circularization. ODNs I−V (Table 1) were 5′-end labeled using [γ-^{32}P]ATP and T4 polynucleotide kinase and then extensively phosphorylated using 1 mM ATP. Ten picomoles of a circularizable ODN and 0.5 pmol of plasmid DNA were incubated in 16 μL of 0.5× TEN buffer (pH 7.4) at 65 °C for 10 min and then slowly cooled to 37 °C. Sixty picomoles (1 μL) of a scaffold ODN VI was added; the mixture was incubated at 37 °C for 30 min after which time 2 μL of 10× ligation buffer and 1 μL (6.7 units) of T4 ligase were added, and the mixture was incubated at 16 °C for 16 h. In an alternative protocol, the ODN−DNA hybridization complex was cooled from 65 to 45 °C, incubated with 60 pmol of scaffold ODN at 45 °C for 30 min, and then incubated with 6.7 units of *Taq* ligase at 45 °C for 4 h.

Electrophoretic Analysis of the Structure of the ODN−DNA Complex. ODN complexes with supercoiled DNA or *Ahd*I−*Alw*NI fragments were separated in a 1.2% agarose gel in TAE buffer [40 mM Tris, 5 mM sodium acetate, and 1 mM EDTA (pH 8.3)]. The gel was stained with EtBr, photographed, dried, and exposed to a PhosphorImager screen for radioactive detection. To verify stable ODN binding, DNA was digested with *Ahd*I and *Alw*NI to release a 480 bp fragment the migration of which in a native 5% polyacrylamide gel was retarded by the bound ODN. The

yield of ODN−DNA complexes was taken as a fraction of the retarded 480 bp fragment relative to the total amount of that fragment in the lane.

Atomic Force Microscopic Analysis of the ODN−DNA Complex. Slowly migrating fragments of ODN II−DNA and ODN V−DNA complexes were excised from a 5% native polyacrylamide gel, and DNA was isolated by the crush and soak method (*25*) followed by purification using a MoBio UltraClean 15 kit (MoBio, Solana Beach, CA). Supercoiled DNA with a biotinylated ODN V label was excised from a 1.2% agarose gel and purified using the MoBio kit. Samples for AFM imaging were prepared in TE buffer [10 mM Tris-HCl (pH 7.9) and 1 mM EDTA]. The samples with the biotinylated probe were complexed with streptavidin (Sigma) in TNM buffer [10 mM Tris-HCl (pH 7.9), 50 mM NaCl, and 10 mM $Mg(OAc)_2$] at a molar DNA:streptavidin ratio of 1:3 for DNA fragments and 1:8 for the plasmid. After incubation for 15 min at room temperature, samples were diluted with TE buffer to a final DNA concentration of 0.3 ng/μL. The AFM imaging procedure, using APS-modified mica as an AFM support, was as described previously (*26*). Briefly, DNA samples (3−5 μL) were placed onto APS-modified mica for 2 min, and then the mica was rinsed with deionized water and dried in an argon flow. Images were acquired in air by a MultiMode SPM NanoScope III system (Veeco/Digital Instruments, Santa Barbara, CA) operating in the tapping mode using OTESPA probes (Digital Instruments). The length, height, and angle measurements were performed with the Femtoscan software (Advanced Technologies Center, Moscow, Russia).

RESULTS

Gel Electrophoresis and Chemical Modification Analyses of the Hybridization Reaction. To test if the DNA unwinding element may serve as a target for site-specific labeling via ODN circularization as outlined in Figure 1, we used pUC derivative plasmid pEV70. Like other pUC vectors, it has an A+T rich sequence in the vicinity of the β-lactamase (ampicillin resistance) gene. At 37 °C, increasing superhelical tension in the plasmid results in unwinding of the A+T rich sequence detected by the CAA reactivity of unpaired adenines and cytosines (Figure 2). A significant extent of DNA unwinding was detected in fraction 5 [superhelical density (σ) = −0.047] which is close to the average superhelical density (σ = −0.05) determined for plasmid DNA isolated from *E. coli*. For an easy use of the described approach by other researchers, the ODN labeling experiments were carried out with superhelical DNA as isolated from bacterial cells.

In most experiments, we used label ODN II that contains an internal 30 nt sequence complementary to one of the strands in the A+T rich plasmid region. After ODN II had hybridized to plasmid DNA, it was ligated into a circular form using scaffold ODN VI (Figure 3A). Panels B−E of Figure 3 show an analysis of the hybridization/ligation reaction products. In an agarose gel, ODN II that did not bind to DNA migrated fast and was detected at the bottom of the gel (Figure 3B,C). A comparison of lane 2 in Figure 3B and lane 2 in Figure 3C with EtBr and radioactive detection, respectively, shows comigration of radioactive label with supercoiled DNA, indicating association of the plasmid with a circularized ODN.

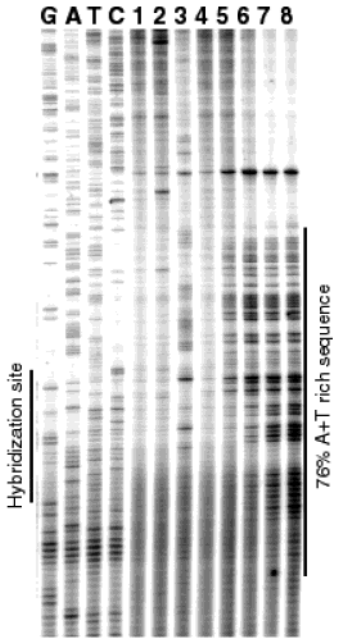

FIGURE 2: Detection of supercoil-induced unwinding in the 97 bp A+T rich sequence of pEV70 by chemical probing at 37 °C. DNA topoisomers were reacted with CAA as described in Experimental Procedures and analyzed by primer extension, and chemically modified unpaired adenines and cytosines in the unwound region were revealed on a 7% denaturing polyacrylamide gel. Superhelical densities of topoisomer preparations were as follows: lane 1, σ = 0; lane 2, σ = −0.019; lane 3, σ = −0.030; lane 4, σ = −0.039; lane 5, σ = −0.047; lane 6, σ = −0.058; lane 7, σ = −0.066; and lane 8, σ = −0.074.

Heating to 65 °C and quick cooling an aliquot of the reaction to dissociate noncircularized ODN did not remove the radioactive label from DNA (lane 3), consistent with ODN catenation. The ODN likely threaded double-stranded DNA since, after the restriction digestion with *Ahd*I and *Alw*NI, it did not slide off the 480 bp DNA fragment that includes the target sequence (lane 4). This conclusion is in agreement with an analysis of the hybridization/ligation reaction products in a polyacrylamide gel (Figure 3D,E). In addition to a normally migrating 480 bp fragment, a fraction of it migrated slower than expected and carried a radioactive label (lanes 2). The extent of fragment retardation was greater than might be explained by a molecular weight increase upon ODN binding. DNA migration in the microporous medium (polyacrylamide) is sensitive to the global DNA shape such as bending. Distortion of the double helix at the ODN threading site results in bending and concomitant slow migration of the DNA fragment, as if it were 780 bp. There was also another, minor retarded species the structure of which will be discussed below in the AFM analysis section. The yield of the ODN−DNA complexes was ~25%.

To gain further insight into the factors that are important for efficient ODN circularization at the target DNA sequence, we used ODN I−III with different lengths of complementarity to the unwound DNA region (40, 30, and 20 nt, Table 1). All ODNs had flanking regions of sufficient length for efficient circularization. To test the importance of ODN diffusion through the unwound region before the actual hybridization occurred, the 30 and 20 nt hybridization sequences were positioned closer to one end of the ODN probe. The 5′-nucleotide-dependent ODN phosphorylation efficiency (*27*) may also influence the yield of circularized

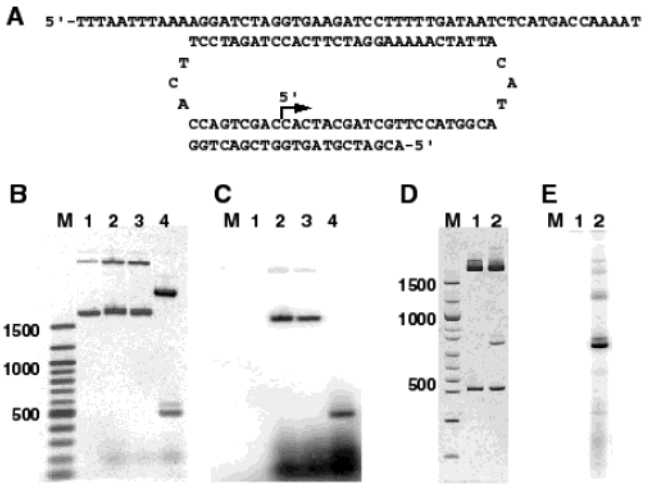

FIGURE 3: Analysis of ODN II circularization reaction products in agarose and polyacrylamide gels. Plasmid pEV70 was hybridized with ODN as described in Experimental Procedures, and the ODN was circularized by the T4 ligase. (B and C) Agarose gel, EtBr staining and radioactivity detection, respectively: lane M, 100 bp size markers; lane 1, untreated DNA, supercoiled DNA migrates just above the 1500 bp marker; lane 2, DNA after ODN circularization reaction carries radioactively labeled ODN; lane 3, like lane 2, but after an additional heating at 65 °C to dissociate unbound ODN; and lane 4, DNA after ODN the circularization reaction and *Ahd*I−*Alw*NI digestion that releases the 480 bp DNA fragment containing the target sequence for ODN. (D and E) Polyacrylamide (5%) gel, EtBr staining and radioactivity detection, respectively. DNA bending upon ODN binding results in a slower migration of the 480 bp DNA fragment: lane M, 100 bp size markers; lane 1, DNA cut with *Ahd*I and *Alw*NI; and lane 2, DNA after the ODN circularization reaction and *Ahd*I−*Alw*NI digestion.

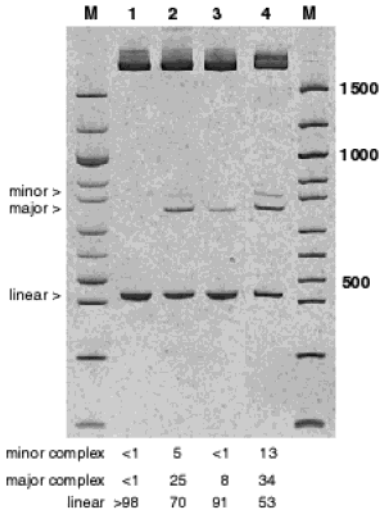

FIGURE 4: Yield of ODN circularization reaction products as a function of ODN length and 5′-terminal nucleotide. DNA was hybridized with several ODNs as described in Experimental Procedures, and the ODNs were circularized by the *Taq* ligase. Fractions of the *Ahd*I−*Alw*NI fragments retarded due to ODN binding were analyzed on a native 5% polyacrylamide gel. ODN hybridization lengths were as follows: 40 nt (lane 1, ODN I), 30 nt (lane 2, ODN II), 20 nt (lane 3, ODN III), and 30 nt (lane 4, ODN IV). ODN II and ODN IV contain 5′-terminal cytosine and adenine, respectively. Fractions of the short fragments without ODN (bottom band) and the two ODN-bound species (middle and top bands) are indicated below the gel.

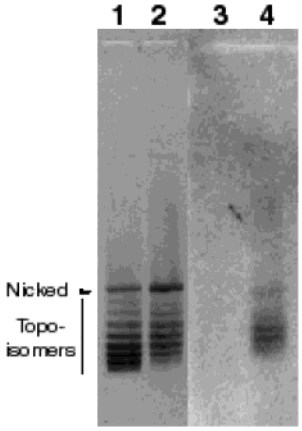

FIGURE 5: Analysis of a change in DNA supercoiling during ODN II circularization from a change in the gel migration of DNA topoisomers. Plasmid pEV70 (0.25 μg) was separated in 1.2% agarose using TAE buffer containing 5 μg/mL chloroquine to resolve DNA topoisomers that differ in the number of superhelical turns. After EtBr detection (lanes 1 and 2), the gel was dried and the radioactivity detected using a PhosphorImager screen (lanes 3 and 4): lanes 1 and 3, nontreated DNA; and lanes 2 and 4, DNA after ODN II circularization.

ODN. To test this, we compared ODNs with 30 nt hybridization sequences that had different 5′-termini. ODN II with a 5′-terminal cytosine had a lower phosphorylation rate than ODN IV with a 5′-terminal adenine (*27*). Figure 4 shows that in the series of 40, 30, and 20 nt hybridization sequences (lanes 1−3), ODN II (lane 2) that may potentially form 30 base pairs with the target DNA was circularized most efficiently (the combined yield of the major and minor ODN−DNA complexes was 30%). This indicates that the hybridization length must be sufficient for stable binding; however, a longer ODN I (lane 1) may not as efficiently diffuse through the unwound loop or wrap several times around the looped-out DNA strand. Replacement of the 5′-cytosine with the 5′-adenine for better phosphorylation and subsequent ligation resulted in a higher yield for the circularization reaction (compare lanes 2 and 4), although the difference was not as great as in the simple 5′-labeling reaction (*27*). The combined yield of the major and minor ODN IV−DNA complexes was almost 50%.

To characterize the local ODN−DNA structure at the hybridization site, we analyzed the number of supercoils in DNA before and after the circularization reaction using agarose gel electrophoresis in the presence of 5 μg/mL chloroquine. Figure 5 shows that after ODN circularization, the topoisomer distribution was shifted upward to a slightly lower negative superhelical density (compare lanes 1 and 2). Even though topoisomers at the bottom of lane 1 partially overlap, they can be reliably counted because topoisomer distributions normally have no more than seven bands, all of which are visible in this lane. The distribution in lane 2 clearly lacks at least one lower band compared with lane 1; therefore, ODN circularization results in DNA unwinding by one or two supercoils. DNA topoisomers that carry radioactively labeled ODN (lane 4) follow the shift detected by EtBr staining (lane 2). Thus, ODN binding relaxes one or two supercoils. In doing so, ODN presumably forms one or two (out of three possible) helical turns with one strand of the DNA target.

Atomic Force Microscopy Analysis of Hybrid Molecules. Atomic force microscopy was used to characterize labeled DNA molecules. Figure 6 shows images of DNA fragments that migrate slowly in a polyacrylamide gel and supposedly contain the ODN II label. Fragments in Figure 6A,C have

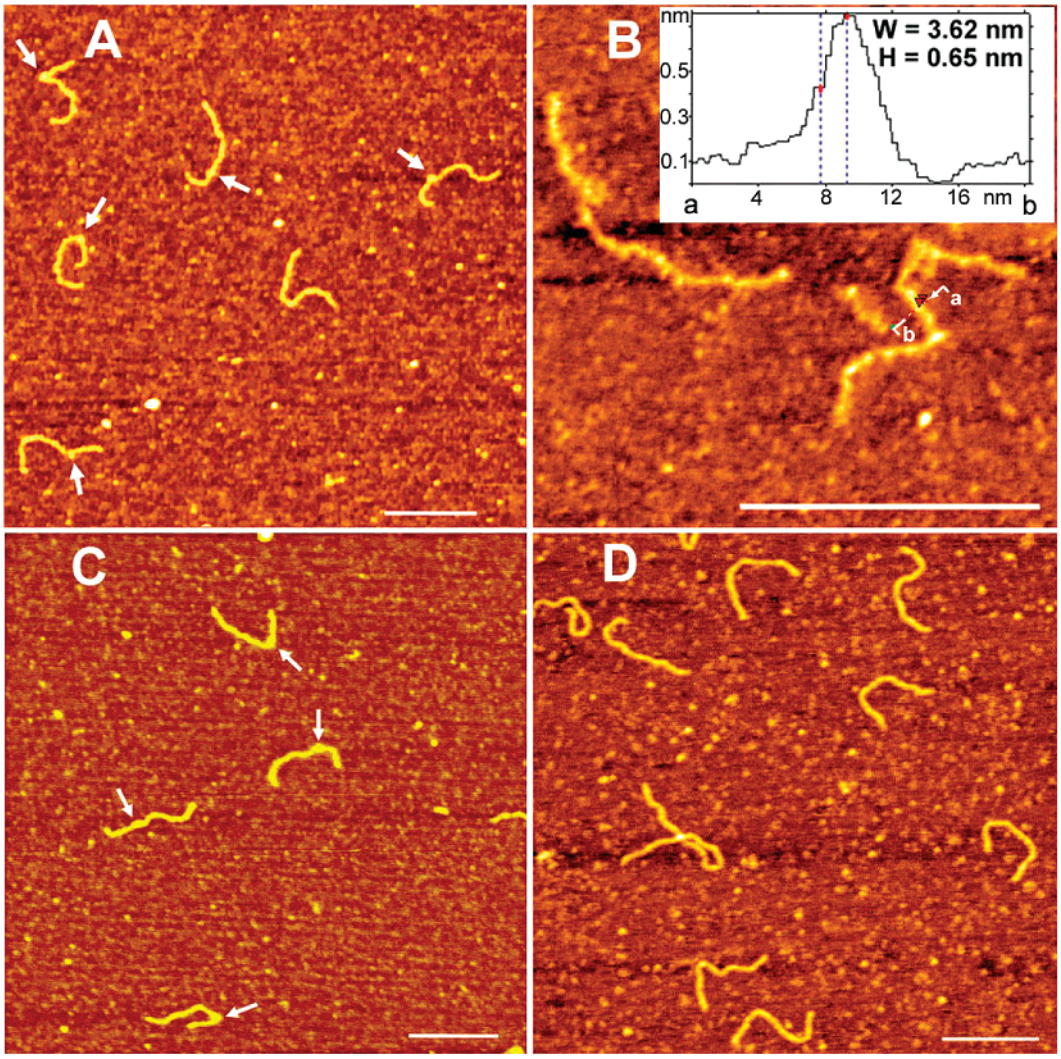

FIGURE 6: AFM analysis of ODN-labeled DNA fragments indicates DNA bending at the ODN binding sites. (A and B) The 480 bp ODN II-labeled DNA fragment migrating the slowest in the polyacrylamide gel. (C) The faster migrating ODN II-labeled DNA fragment. (D) The control, unlabeled DNA fragment that migrates in a gel as expected. The inset in panel B demonstrates the AFM resolution by showing a <4 nm thickness of a DNA molecule. Bars are 100 nm long.

clearly identified bulges (indicated with arrows) that are asymmetrically positioned relative to the fragment ends. Such bulges are not present in a control image of the normally migrating fragment (Figure 6D). In a high-resolution image of the slowly migrating fragment (Figure 6B), the bulges look more like loops, although their fine structure cannot be resolved. Remarkably, the width of DNA in this image, measured as a half-width of the cross-section peaks, is less than 4 nm, allowing D-loop detection without using any specific marker.

DNA fragments carrying circularized ODN II migrated in a polyacrylamide gel as two distinct species (Figures 3D,E and 4). The end−label distances measured for the long arms in both types of slowly migrating species are shown in Figure 7A,B alongside the contour lengths of the fragments. The mean numbers for both parameters are given in Table 2. The contour lengths of the two fragments are very similar. The end−label distances are very similar as well, which indicates that the label positions in the two species are identical. By an experimental design, the A+T rich hybridization site is 313−342 bp from the *Alw*NI site, with the center at 68% of the contour length of the *Ahd*I−*Alw*NI fragment. This is in a perfect agreement with label positions determined from AFM images that are at 69 and 67% of the lengths of the *Ahd*I−*Alw*NI fragments migrating in the upper and lower retarded bands, respectively.

An interesting feature of the ODN−DNA complexes is the kink introduced at the label position. Similar to our previous AFM data on DNA fragments containing three-way junctions (*26*), we suggested that the difference in gel mobility of DNA fragments carrying the circular ODN was due to the difference in the kink angle. To verify this suggestion, we measured the kink angle for both slowly migrating DNA fragments. The angle distributions (Figure 7C,D) and the mean angle values (Table 2) confirm that the most retarded fragment is much more bent than the less retarded one.

Although the ODN labels can be reliably distinguished in isolated fragments, their unambiguous and routine identification in supercoiled plasmids is not straightforward. To facilitate label identification, complexes of biotinylated ODN V with DNA were bound to streptavidin to increase the visibility of the looped regions (Figure 8A). In addition to streptavidin−DNA binding at a 1:1 ratio, anchoring of several DNA fragments by one streptavidin tetramer was sometimes observed. An inset in Figure 8A shows a zoomed

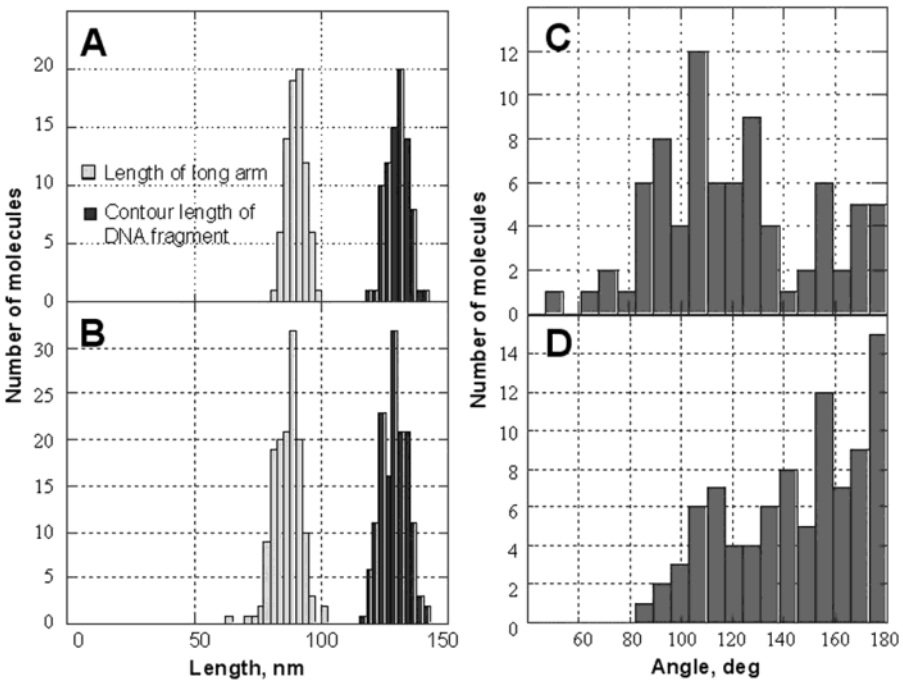

FIGURE 7: Characterization of the ODN−DNA complex structure. End−label distances and contour lengths for the slower (A) and faster (B) migrating 480 bp ODN II-labeled DNA fragments indicate ODN binding at the expected target site. The slower (C) and faster (D) migrating ODN II-labeled DNA fragments differ in the extent of DNA bending as demonstrated by the angles between the two DNA arms outgoing from the label positions.

Table 2: Structural Characteristics of the *Ahd*I−*Alw*NI Fragments of pEV70 Carrying Circularized Oligonucleotides[a]

	long arm (nm)	contour length (nm)	interarm angle (deg)
minor complex	90.1 ± 3.6	130.1 ± 4.2	123.9 ± 31.8
major complex	86.7 ± 5.5	128.6 ± 5.0	146.6 ± 26.1
major complex with streptavidin	85.7 ± 4.9	129.3 ± 5.3	149.8 ± 29.4

[a] Definitions of the minor and major complexes are the same as in Figure 4. The numbers of DNA molecules analyzed for each determination were between 80 and 165.

image of a "trimer". An approximately 2:1 ratio of the short and long arm lengths indicates a high specificity of DNA labeling with streptavidin. The mean values for the long arm lengths (Table 2) are very close to those determined in the absence of streptavidin. A comparison of cross sections of DNA and bound streptavidin (Figure 8B) illustrates the contrast enhancement by streptavidin binding. The protein appears in the AFM images as a bright formation 2 times wider and 4 times higher than DNA.

Figure 8C shows an image of the plasmid that was labeled with a biotinylated ODN V, complexed with streptavidin, and then deposited on mica from a low-salt TE buffer. Unambiguously identified streptavidin molecules are indicated with arrows. The population of such complexes, 24.8% of the 754 molecules that were analyzed, is very close to the yield of the complexes estimated from the gel electrophoresis data (26.4%). The control sample with a nonbiotinylated probe is shown in Figure 8D. There are no streptavidin molecules bound to DNA, although protein molecules away from DNA can be identified. An extensive analysis of control images (155 molecules) showed less than 2% of nonspecific complexes. In AFM images for DNA deposited from the Mg-containing buffer where supercoiled DNA becomes plectonemic, 82% of the molecules have the streptavidin label in the apical position (Figure 9), which is consistent with DNA bending at the ODN binding site as observed in the electrophoretic experiments.

DISCUSSION

The results presented in this paper show that the proposed approach of DNA labeling at easily unwinding sites is feasible. An obvious choice of such sites are A+T regions in supercoiled DNA that are prone to unwinding, especially at elevated temperatures. This approach allowed site-specific labeling of supercoiled DNA with up to 50% yield. The narrow distributions of the end−label distances (Figure 7A,B), derived from the AFM images, provide evidence of very well defined label positions in the DNA sequences. This is consistent with ODN threading the unwound DNA loop and forming a double-helical structure with one of the DNA strands. DNA is base-paired everywhere but the hybridization site, and this prevents the ODN from moving around the plasmid. Another indication of ODN threading is that it does not dissociate from DNA upon heating. The bound and circularized ODN presumably forms a few turns of helix with the complementary strand of unwound DNA. The other DNA strand remains unpaired so that the resultant loop entails relaxation of several supercoils. As can be inferred from the topoisomer distributions for plasmids with and without bound ODN (Figure 5), one or two supercoils are relaxed. The specific binding mode when the ODN threads the double helix results in DNA bending detected in polyacrylamide gel (Figures 3 and 4) and AFM images (Figure 6). A polyacrylamide gel analysis (Figure 4) shows that there are two ODN-labeled DNA species, the minor species being more apparent as the yield of labeled DNA increases. The minor species likely reflects an ODN hybridization mode somewhat different than that in the major ODN−DNA complex. It is possible that the two hybridization modes may

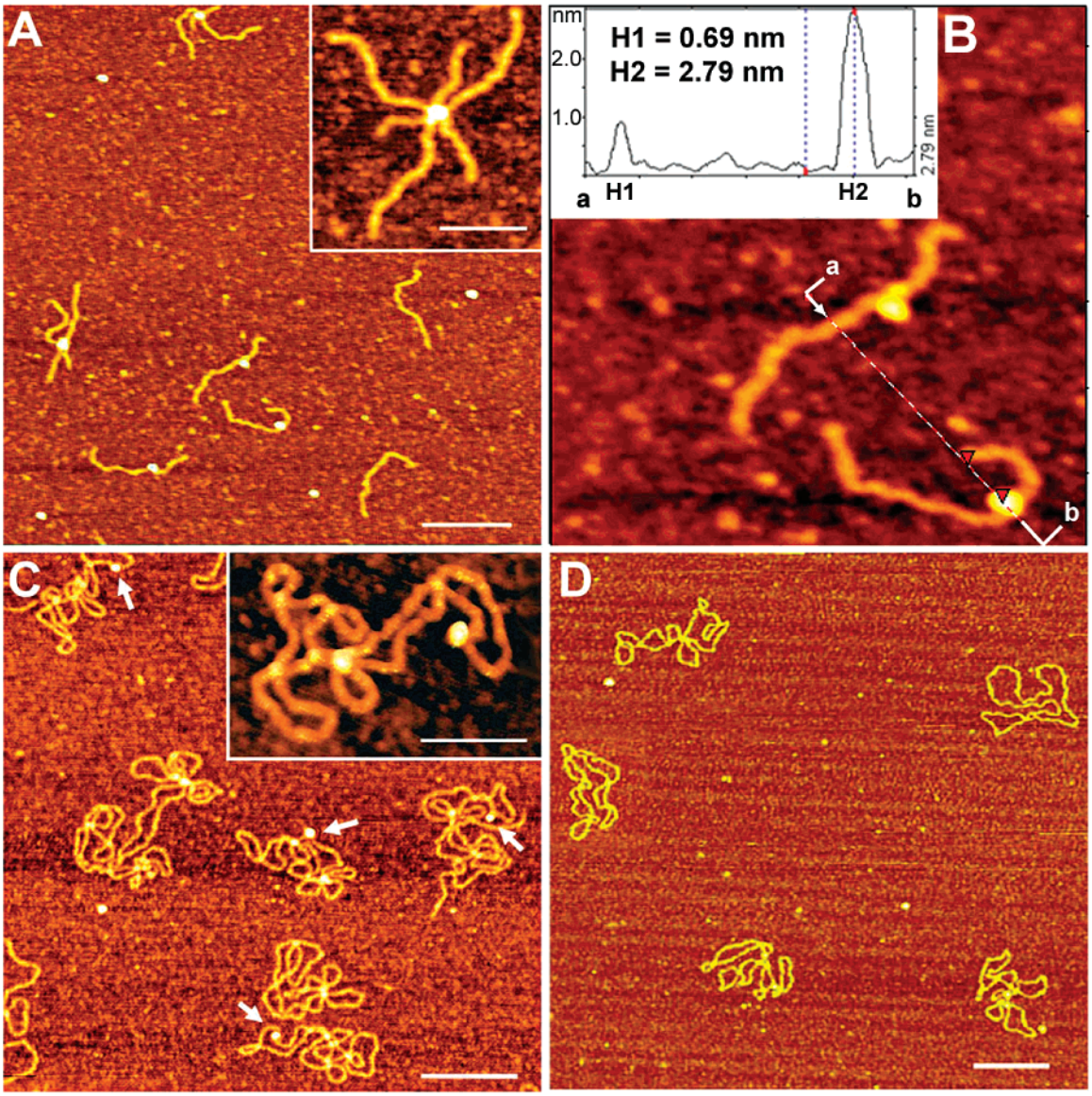

FIGURE 8: Detection of the ODN labeling sites by streptavidin binding. (A) DNA fragments with bound ODN V and streptavidin. Occasionally, multiple-ODN binding to a single streptavidin tetramer was observed (inset). (B) Cross-section analysis shows a severalfold height difference between the DNA molecule and DNA complexed with streptavidin. (C) Supercoiled DNA with bound streptavidin indicated by arrows. After protein binding, DNA was adjusted to and deposited from TE buffer. (D) Control sample of the same plasmid without ODN but incubated with streptavidin. Bars are 100 nm long, and 50 nm in insets.

correspond to two different numbers of helical turns that ODN makes with the unwound DNA strand. AFM images (Figure 9) also show a global positioning effect in that the bend tends to occupy an apical position in supercoiled DNA similar to an A-tract bend (*28*).

The proposed approach utilizes stable ODN hybridization to DNA strands made unpaired below their melting temperature by the torsional stress in supercoiled DNA. Stable strand separation below the melting temperature in relaxed or linear DNA that lacks the torsional stress is impossible. In the melting temperature interval, ODN cannot stably bind to unpaired DNA strands. Therefore, the proposed approach will work efficiently for only supercoiled DNA. Our approach requires no specific nucleotide motif for ODN binding to supercoiled DNA by strand invasion. Although the ODN hybridization efficiency is higher at the sites where duplex DNA is destabilized such as the A+T rich sequences (this work) or cruciform-forming sites (*17*), significant ODN uptake by mixed sequence DNA was also observed at elevated temperatures (*14*, *15*). Thus, albeit at different efficiencies, ODNs may be used to target various sequences in plasmids.

There are many practical applications of stable site-specific ODN binding to supercoiled DNA. Biotin−streptavidin labels may serve as site-specific markers that may be used to identify the relative positions of other sites of interest in circular DNA (*1*). For visualization techniques such as electron and atomic force microscopies, such markers would allow reliable mapping of protein binding sites and local alternative structures as well as monitoring of structural dynamics of DNA molecules in real time (*2*, *3*). For example, intermediates of supercoil-driven local structures such as cruciforms and intramolecular triplex (*2*, *3*) or protein binding to the supercoil-driven Z-DNA and cruciforms (*4*, *5*) can be unambiguously identified with the help of sequence-specific markers in circular DNA. Biotin−streptavidin binding may also be used for a stable site-specific anchoring of DNA molecules to mica support used in atomic force microscopy.

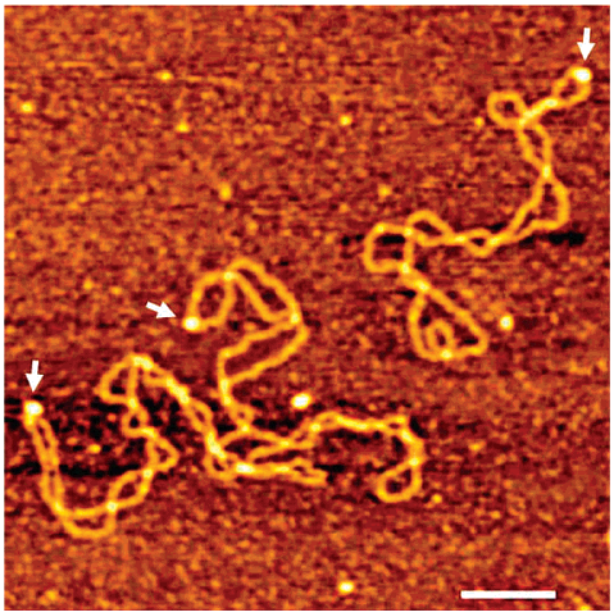

FIGURE 9: ODN circularization at the A+T rich sequence produces DNA bend that tends to occupy an apical position in supercoiled DNA. AFM images show a complex of supercoiled DNA with ODN V that after streptavidin binding in Mg-containing buffer was deposited from the same buffer. The bar is 50 nm long.

Site-specific ODN reactions with DNA may also be used to prepare conjugates for the antibody- and nuclear localization signal peptide-mediated gene delivery, as well as for monitoring the intracellular distribution of fluorescently labeled DNA (*29*−*31*). DNA curvature plays important roles in transcription, DNA replication, and recombination (*32*). In particular, DNA bending may bring distant protein binding sites into proximity, as in transcription initiation, or properly position DNA sites, as in site-specific recombination (*33*, *34*). Site-specific DNA bending induced by ODN uptake may provide a basis for the development of strategies of interference with such processes by modulating the extent of intrinsic and protein-induced DNA curvature.

To summarize, our experiments represent an important step in the development of site-specific approaches to labeling circular DNA. We made use of ODN uptake by plasmids under negative torsional tension. ODN circularization via templated ligation results in its highly localized threading between the two strands of duplex DNA. Site-specific labels allow visualization techniques, such as electron and atomic force microscopies, to reliably map protein binding sites, identify local alternative structures in supercoiled DNA, and monitor structural dynamics of DNA molecules in real time. Site-specific ODN reactions with DNA may also be used to prepare conjugates for the antibody- and nuclear localization signal peptide-mediated gene delivery, and for monitoring the intracellular distribution of fluorescently labeled DNA. Site-specific DNA bending induced by the ODN uptake may be potentially used to modulate the extent of DNA curvature that plays important roles in the initiation of transcription, DNA replication, and recombination.

ACKNOWLEDGMENT

We thank Elena Oussatcheva for construction of plasmid pEV70 and Luda Shlyakhtenko for critical advice in the course of the AFM studies and useful comments on the paper.

REFERENCES

1. Pfannschmidt, C., and Langowski, J. (1998) Superhelix organization by DNA curvature as measured through site-specific labeling, *J. Mol. Biol. 275*, 601−611.
2. Shlyakhtenko, L. S., Potaman, V. N., Sinden, R. R., and Lyubchenko, Y. L. (1998) Structure and dynamics of supercoil-stabilized DNA cruciforms, *J. Mol. Biol. 280*, 61−72.
3. Tiner, W. J., Potaman, V. N., Sinden, R. R., and Lyubchenko, Y. L. (2001) The structure of intramolecular DNA triplex: atomic force microscopy studies, *J. Mol. Biol. 314*, 353−357.
4. Herbert, A., Schade, M., Lowenhaupt, K., Alfken, J., Schwartz, T., Shlyakhtenko, L. S., Lyubchenko, Y. L., and Rich A. (1998) The Zα domain from human ADAR1 binds to the Z-DNA conformer of many different sequences, *Nucleic Acids Res. 26*, 3486−3493.
5. Soldatenkov, V. A., Chasovskikh, S., Potaman, V. N., Trofimova, I., Smulson, M. E., and Dritschilo, A. (2002) Transcriptional repression by binding of poly(ADP-ribose) polymerase to promoter sequences, *J. Biol. Chem. 277*, 665−670.
6. Shlyakhtenko, L. S., Gall, A. A., Weimer, J. J., Hawn, D. D., and Lyubchenko, Y. L. (1999) Atomic force microscopy imaging of DNA covalently immobilized on a functionalized mica substrate, *Biophys. J. 77*, 568−576.
7. Pfannschmidt, C., Schaper, A., Heim, G., Jovin, T. M., and Langowski, J. (1996) Site-specific labeling of superhelical DNA by triple helix formation and psoralen crosslinking, *Nucleic Acids Res. 24*, 1702−1709.
8. Escude, C., Garestier, T., and Helene, C. (1999) Padlock oligonucleotides for duplex DNA based on sequence-specific triple helix formation, *Proc. Natl. Acad. Sci. U.S.A. 96*, 10603−10607.
9. Roulon, T., Helene, C., and Escude, C. (2001) A ligand-modulated padlock oligonucleotide for supercoiled plasmids, *Angew. Chem., Int. Ed. 40*, 1523−1526.
10. Roulon, T., Coulaud, D., Delain, E., Le Cam, E., Helene, C., and Escude, C. (2002) Padlock oligonucleotides as a tool for labeling superhelical DNA, *Nucleic Acids Res. 30*, e12.
11. Kuhn, H., Demidov, V. V., and Frank-Kamenetskii, M. D. (1999) Topological links between duplex DNA and a circular DNA single strand, *Angew. Chem., Int. Ed. 38*, 1446−1449.
12. Demidov, V. V., Kuhn, H., Lavrentieva-Smolina, I. V., and Frank-Kamenetskii, M. D. (2001) Peptide nucleic acid-assisted topological labeling of duplex DNA, *Methods 23*, 123−131.
13. Demidov, V. V., Protozanova, E., Izvolsky, K. I., Price, C., Nielsen, P. E., and Frank-Kamenetskii, M. D. (2002) Kinetics and mechanism of the DNA double helix invasion by pseudocomplementary peptide nucleic acids, *Proc. Natl. Acad. Sci. U.S.A. 99*, 5953−5958.
14. Holloman, W. K., Wiegand, R., Hoessli, C., and Radding, C. M. (1975) Uptake of homologous single-stranded fragments by superhelical DNA: a possible mechanism for initiation of genetic recombination, *Proc. Natl. Acad. Sci. U.S.A. 72*, 2394−2398.
15. Beattie, K. L., Wiegand, R. C., and Radding, C. M. (1977) Uptake of homologous single-stranded fragments by superhelical DNA. II. Characterization of the reaction, *J. Mol. Biol. 116*, 783−803.
16. Corey, D. R., and Schultz, P. G. (1989) The sequence-selective hydrolysis of duplex DNA by an oligonucleotide-directed nuclease, *J. Am. Chem. Soc. 111*, 8523.
17. Corey, D. R., Munoz-Medellin, D., and Huang, A. (1995) Strand-invasion by oligonucleotide-nuclease conjugates, *Bioconjugate Chem. 6*, 93−100.
18. Kowalski, D., Natale, D. A., and Eddy, M. J. (1988) Stable DNA unwinding, not "breathing", accounts for single-strand-specific nuclease hypersensitivity of specific A+T-rich sequences, *Proc. Natl. Acad. Sci. U.S.A. 85*, 9464−9468.
19. Lyubchenko, Y. L., and Shlyakhtenko, L. S. (1988) Early melting of supercoiled DNA, *Nucleic Acids Res. 16*, 3269−3281.
20. Voloshin, O. N., Shlyakhtenko, L. S., and Lyubchenko, Y. L. (1989) Localization of melted regions in supercoiled DNA, *FEBS Lett. 243*, 377−380.
21. Kohwi-Shigematsu, T., and Kohwi, Y. (1990) Torsional stress stabilizes extended base unpairing in suppressor sites flanking immunoglobulin heavy chain enhancer, *Biochemistry 29*, 9551−9560.
22. Hancock, R. (1974) Interphase chromosomal deoxyribonucleoprotein isolated as a discrete structure from cultured cells, *J. Mol. Biol. 86*, 649−663.

23. Potaman, V. N., and Sinden, R. R. (1998) Stabilization of triple/single strand (H-DNA) structure by cationic peptides, *Biochemistry 37*, 12952−12961.
24. Oussatcheva, E. A., Shlyakhtenko, L. S., Glass, R., Sinden, R. R., Lyubchenko, Y. L., and Potaman, V. N. (1999) Structure of branched DNA molecules: gel retardation and atomic force microscopy studies, *J. Mol. Biol. 292*, 75−86.
25. Sambrook, J., Fritsch, E. F., and Maniatis, T. (1989) *Molecular Cloning: A Laboratory Manual*, Cold Spring Harbor Laboratory Press, Plainview, NY.
26. Shlyakhtenko, L. S., Potaman, V. N., Sinden, R. R., Gall, A. A., and Lyubchenko, Y. L. (2000) Structure and dynamics of three-way DNA junctions: atomic force microscopy studies, *Nucleic Acids Res. 28*, 3472−3477.
27. Van Houten, V., Denkers, F., van Dijk, M., van den Brekel, M., and Brekenhoff, R. (1998) Labeling efficiency of oligonucleotides by T4 polynucleotide kinase depends on 5′-nucleotide, *Anal. Biochem. 265*, 386−389.
28. Laundon, C. H., and Griffith, J. D. (1988) Curved helix segments can uniquely orient the topology of supertwisted DNA, *Cell 52*, 545−549.
29. Poncet, P., Panczak, A., Goupy, C., Gustafsson, K., Blanpied, C., Chavanel, G., Hirsch, R., and Hirsch, F. (1996) Antifection: an antibody-mediated method to introduce genes into lymphoid cells in vitro and in vivo, *Gene Ther. 3*, 731−738.
30. Sebestyen, M. G., Ludtke, J. J., Bassik, M. C., Zhang, G., Budker, V., Lukhtanov, E. A., Hagstrom, J. E., and Wolff, J. A. (1998) DNA vector chemistry: the covalent attachment of signal peptides to plasmid DNA, *Nat. Biotechnol. 16*, 80−85.
31. Zelphati, O., Liang, X., Hobart, P., and Felgner, P. L. (1999) Gene chemistry: functionally and conformationally intact fluorescent plasmid DNA, *Hum. Gene Ther. 10*, 15−24.
32. Sinden, R. R. (1994) *DNA Structure and Function*, Academic Press, San Diego.
33. Kohwi, Y., and Panchenko, Y. (1993) Transcription-dependent recombination induced by triple-helix formation, *Genes Dev. 7*, 1766−1778.
34. Shlyakhtenko, L. S., Hsieh, P., Grigoriev, M., Potaman, V. N., Sinden, R. R., and Lyubchenko, Y. L. (2000) A cruciform structural transition provides a molecular switch for chromosome structure and dynamics, *J. Mol. Biol. 296*, 1169−1173.

BI026402W